



Cite this: *Dalton Trans.*, 2016, **45**, 6548

Charge transfer complexes of fullerenes containing $C_{60}^{\cdot-}$ and $C_{70}^{\cdot-}$ radical anions with paramagnetic $Co^{II}(dppe)_2Cl^+$ cations ($dppe$: 1,2-bis(diphenylphosphino)ethane) †

Dmitri V. Konarev,^{*a} Sergey I. Troyanov,^b Akihiro Otsuka,^c Hideki Yamochi,^c Gunzi Saito^{d,e} and Rimma N. Lyubovskaya^a

The reduction of $Co^{II}(dppe)Cl_2$ with sodium fluorenone ketyl produces a red solution containing the Co^I species. The dissolution of C_{60} in the obtained solution followed by the precipitation of crystals with hexane yields a salt $\{Co^I(dppe)_2\}^+(C_{60}^{\cdot-}) \cdot 2C_6H_4Cl_2$ and a novel complex $\{Co(dppe)_2Cl\}(C_{60})$ (**1**). With C_{70} , only the crystals of $\{Co(dppe)_2Cl\}(C_{70}) \cdot 0.5C_6H_4Cl_2$ (**2**) are formed. Complex **1** contains zig-zag fullerene chains whereas closely packed double chains are formed from fullerenes in **2**. According to the optical spectra and magnetic data charge transfer occurs in both **1** and **2** with the formation of the $Co^{II}(dppe)_2Cl^+$ cations and the $C_{60}^{\cdot-}$ or $C_{70}^{\cdot-}$ radical anions. In spite of the close packing in crystals, $C_{60}^{\cdot-}$ or $C_{70}^{\cdot-}$ retain their monomeric form at least down to 100 K. The effective magnetic moments of **1** and **2** of 1.98 and $2.27\mu_B$ at 300 K, respectively, do not attain the value of $2.45\mu_B$ expected for the system with two non-interacting $S = 1/2$ spins at full charge transfer to fullerenes. Most probably diamagnetic $\{Co^I(dppe)_2Cl\}^0$ and neutral fullerenes are partially preserved in the samples which can explain the weak magnetic coupling of spins and the absence of fullerene dimerization in both complexes. The EPR spectra of **1** and **2** show asymmetric signals approximated by several lines with g -factors ranging from 2.0009 to 2.3325. These signals originate from the exchange interaction between the paramagnetic $Co^{II}(dppe)_2Cl^+$ cations and the fullerene $^{\cdot-}$ radical anions.

Received 25th November 2015,
Accepted 19th February 2016

DOI: 10.1039/c5dt04627k

www.rsc.org/dalton

Introduction

Ionic compounds of fullerenes possess promising conducting and magnetic properties.^{1–4} Crystalline samples of these compounds are generally prepared using organic or solvated metal cations.^{5,6} Metallocenes are strong donor molecules to give charge-transfer (CT) complexes composed of mono- to tri-anionic fullerenes.^{7–10} Also, by employing extra reducing agents such as alkali metals or tetrakis(dimethylamino)ethylene

(TDAE), anionic fullerene complexes with organometallic cations are prepared. The latter method provided complexes with $\{(Ph_3P)_3Au\}^+$,¹¹ $Co^I(dppe)_2^+$ (ref. 12) and positively charged Ph_3P -containing gold clusters,¹³ for example. The organometallic cations can introduce paramagnetic centers into the ionic fullerene systems.

In our previous work we studied coordination compounds of fullerene C_{60} with cobalt in zero oxidation state containing Ph_3P and diphosphine ligands (including 1,2-bis(diphenylphosphino)ethane, $dppe$) and in some cases benzonitrile.^{14–16} In this work we studied the interaction of fullerenes C_{60} and C_{70} with $Co(dppe)_2Cl$ prepared by the reduction of $Co^{II}(dppe)Cl_2$ with sodium fluorenone ketyl. Crystalline $\{Co(dppe)_2Cl\}(C_{60})$ (**1**) and $\{Co(dppe)_2Cl\}(C_{70}) \cdot 0.5C_6H_4Cl_2$ (**2**) compounds were obtained together with the previously studied salt $\{Co^I(dppe)_2\}^+(C_{60}^{\cdot-}) \cdot 2C_6H_4Cl_2$.¹² We present crystal structures, and optical and magnetic properties of these complexes. Compound **2** is a rare example of an ionic fullerene structure containing monomeric $C_{70}^{\cdot-}$ radical anions while they form single-bonded $(C_{70}^{\cdot-})_2$ dimers^{17–19} in most of the anion radical salts.

^aInstitute of Problems of Chemical Physics RAS, Chernogolovka, Moscow region, 142432 Russia. E-mail: konarev3@yandex.ru

^bChemistry Department, Moscow State University, Leninskie Gory, 119991 Moscow, Russia

^cResearch Center for Low Temperature and Materials Sciences, Kyoto University, Sakyo-ku, Kyoto 606-8501, Japan

^dFaculty of Agriculture, Meijo University, 1-501 Shiogamaguchi, Tempaku-ku, Nagoya 468-8502, Japan

^eToyota Physical and Chemical Research Institute, 41-1, Yokomichi, Nagakute, Aichi 480-1192, Japan

† Electronic supplementary information (ESI) available: IR spectra of **1** and **2**. CCDC 1437134 and 1437135. For ESI and crystallographic data in CIF or other electronic format see DOI: 10.1039/c5dt04627k

Results and discussion

Synthesis

As summarized in Scheme 1, the first reduction potentials for fullerenes C_{60} and C_{70} are -0.44 V and -0.41 V, respectively, in dichloromethane vs. SCE. The second reduction wave is observed at -0.82 and -0.80 V vs. SCE, respectively, in the same solvent.²⁰ The $\{Co^{II}(dppe)_2(CH_3CN)\}^{2+}$ cations can be reduced electrochemically to $\{Co^I(dppe)_2\}^+$ at -0.70 V vs. Fe^+/Fe (-0.275 V vs. SCE).²¹ Previously we used tetrakis(dimethylamino)-ethylene (TDAE) as the reductant for $Co^{II}(dppe)Br_2$ and C_{60} .¹² TDAE with the first oxidation potential of $E^{+/0} = -0.75$ V vs. SCE²² generates the Co^I species and $C_{60}^{\cdot-}$ in solution which cocrystallize to form the $\{Co^I(dppe)_2\}^+\{C_{60}^{\cdot-}\} \cdot 2C_6H_4Cl_2$ salt.¹² While the $Co^I(dppe)_2^+$ cation has an odd $S = 1$ or $S = 0$ spin state, only the $C_{60}^{\cdot-}$ signal is observed in the EPR spectrum of this salt. Further reduction of $Co^I(dppe)_2^+$ to $Co^0(dppe)_2$ by TDAE is not possible (Scheme 1) since the conversion takes place at a more negative redox potential of -1.56 V vs. Fe^+/Fe (-1.135 V vs. SCE).²¹ The $Co^I(dppe)_2^+$ cation is also too weak a donor to reduce $C_{60}^{\cdot-}$ to C_{60}^{2-} .

Sodium fluorenone ketyl (fluorenone $^{\cdot-}$)(Na^+) is a stronger reducing agent than TDAE (Scheme 1) with the first oxidation potential of about -1.30 V vs. $Ag/AgCl$ or (-1.255 V vs. SCE).²³ Therefore, this ketyl can also reduce $Co^{II}(dppe)Cl_2$ to generate the Co^I species. Potentially it can also reduce $Co^{II}(dppe)Cl_2$ to the Co^0 species but such a redox process is hindered in non-polar *o*-dichlorobenzene.

In this study, the formation of Co^I species was detected by the color change of the reaction mixture from the green color of $Co^{II}(dppe)Cl_2$ to red during the reduction with sodium fluorenone ketyl. After the removal of unreacted sodium fluorenone ketyl by filtration, the generated $Co^I(dppe)_n^+$ ($n = 1, 2$) was treated with neutral fullerenes. $Co^I(dppe)_2Cl$ is rather a strong donor and potentially it can reduce fullerenes providing the CT complexes composed of $Co^{II}(dppe)_2^{2+}$ and $C_{60}^{\cdot-}$ or $C_{70}^{\cdot-}$ radical anions. While the main product of this reaction was $\{Co(dppe)_2Cl\}(C_{60})$ (**1**), the $\{Co^I(dppe)_2\}^+\{C_{60}^{\cdot-}\} \cdot 2C_6H_4Cl_2$ salt¹² is also crystallized in 20% yield. The $\{Co(dppe)_2Cl\}(C_{70}) \cdot 0.5C_6H_4Cl_2$ (**2**) complex crystallized exclusively with C_{70} .

Optical properties

The IR spectra of **1** and **2** are listed in Table S1† and are shown in Fig. 1S and 2S.† The spectra practically seem to be the

superposition of the absorption bands of $Co(dppe)_2Cl$ and fullerene anions $C_{60}^{\cdot-}$ or $C_{70}^{\cdot-}$. Neutral fullerene C_{60} shows four F_{1u} mode IR bands at 527, 576, 1183, and 1429 cm^{-1} (denoted as $F_{1u}(1)$ to $F_{1u}(4)$, respectively).^{5,24,25} While other bands exhibit only a few cm^{-1} shifts, the $F_{1u}(4)$ mode shows a 37 cm^{-1} red shift when C_{60} is charged -1 . The strong absorption band observed at 1393 cm^{-1} for **1** unambiguously indicates the formation of $C_{60}^{\cdot-}$. The coexistence of partially reduced or neutral C_{60} cannot be confirmed from the IR spectrum since $Co(dppe)_2Cl$ has intense absorption bands at 1433 and 530 cm^{-1} which coincide with those of neutral C_{60} . A similar situation is observed for complex **2** containing C_{70} (Table S1†).

The UV-visible-NIR spectra of **1** and **2** are shown in Fig. 1. The absorption bands in the spectrum of **1** at 38000, 29700 cm^{-1} (262, 334 nm) and the weaker band at 16 860 cm^{-1} (612 nm) can be attributed to C_{60} whereas the bands in the NIR range at 10 650 and 9240 cm^{-1} (948, 1087 nm) (Fig. 1a) show the presence of $C_{60}^{\cdot-}$.^{5,6} The broad low-energy band of relatively weak intensity at about 7660 cm^{-1} (1300 nm) (Fig. 1a) can be ascribed to the CT transition between fullerenes or the $Co(dppe)_2Cl$ and fullerene species. Similarly, absorption bands in the spectrum of **2** at 26 000 and 20 840 cm^{-1} (382 and 480 nm) are ascribed to C_{70} . The broad absorption band in the NIR range can be reproduced by two Gaussian curves with maxima at about 9900 and 7500 cm^{-1} (1010 and 1330 nm, Fig. 1b and 2). The position of the latter band is close to that in the solution spectrum of monomeric $C_{70}^{\cdot-}$.^{5,6,26} It should be noted that generally C_{70} monoanions form singly bonded $(C_{70}^{\cdot-})_2$ dimers in solids to show two bands in the NIR range at about 11 360 and 8200 cm^{-1} (880 and 1220 nm, Fig. 2).^{17–19} The strong shift of the $(C_{70}^{\cdot-})_2$ band at 880 nm to 1010 nm in the spectrum of **2** proves the failure of dimer formation in **2**. So far, monomeric $C_{70}^{\cdot-}$ are preserved only in the $(Ph_4P^+)_2(C_{70}^{\cdot-})(I^-)$ salt due to the long distances between fullerenes.²⁷ The broad band at about 9900 cm^{-1} (1010 nm) can be attributed to the CT between fullerenes or the $Co(dppe)_2Cl$ and the fullerene species. Low energy CT bands (*ca.* 2000–5000 cm^{-1}) which correspond to the Drude type reflectivity spectra characteristic of metals are not observed in the spectra of both **1** and **2**.

Fluorenone	TDAE	$\{Co^{II}(dppe)_2AN\}^{2+}$	C_{60}	C_{70}
		$\frac{2+/+}{-0.275\text{ V}}$	$\frac{0/-}{-0.44\text{ V}}$	$\frac{0/-}{-0.41\text{ V}}$
	$\frac{0/+}{-0.75\text{ V}}$		$\frac{-2/-}{-0.82\text{ V}}$	$\frac{-2/-}{-0.80\text{ V}}$
		$\frac{+/0}{-1.135\text{ V}}$		
	$\frac{0/-}{-1.255\text{ V}}$			

Scheme 1 Redox potentials of the components used in the synthesis of $Co(dppe)$ -fullerene complexes. All potentials are given vs. SCE.

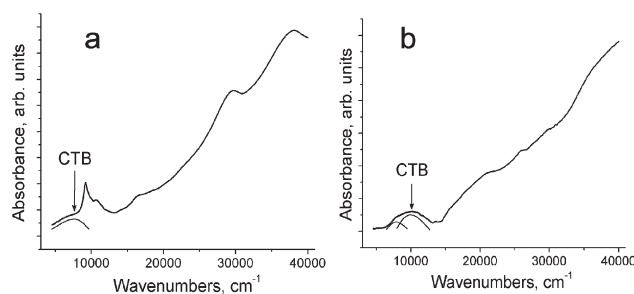


Fig. 1 Spectra of **1** (a) and **2** (b) in the UV-visible-NIR range measured at room temperature using KBr pellets prepared under anaerobic conditions.



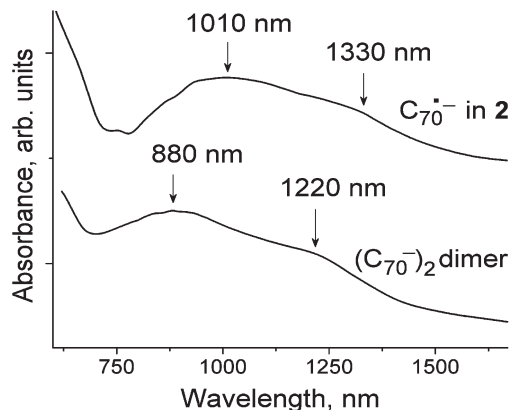


Fig. 2 The comparison of visible-NIR spectra of the $C_{70}^{\cdot-}$ radical anions in **2** (upper spectrum) and the $(C_{70}^{\cdot-})_2$ dimers in the complex $(Cp_2Co^+)_2(C_{70}^{\cdot-})_2 \cdot 2C_6H_4Cl_2$ (lower spectrum).⁸

Crystal structures

$\{Co(dppe)_2Cl\}(C_{60})$ (**1**) contains closely packed zigzag fullerene chains arranged along the *c* axis with equal interfullerene center-to-center (ctc) distances of 9.97 Å. This distance is noticeably shorter than the van der Waals (vdW) diameter of C_{60} (10.18 Å) and multiple vdW $C\cdots C$ contacts are formed between fullerenes (shown by green dashed lines in Fig. 3a). Fullerene chains are isolated (Fig. 3b), and the shortest ctc interfullerene distance between the neighboring chains is 12.53 Å.

Each $Co(dppe)_2Cl$ unit is surrounded by four C_{60} cages (Fig. 3c). Nearly spherical C_{60} is inserted into the cavities formed by four phenyl substituents of $Co(dppe)_2Cl$, and multiple vdW $C_6H(Co(dppe)_2Cl)\cdots C(C_{60})$ contacts are formed. One of the four surrounding fullerenes forms short $Cl(Co(dppe)_2Cl)\cdots C(C_{60})$ contacts of the 2.998–3.107 Å length. The shortest distances (5.22–5.41 Å) between cobalt and the C_{60} carbon atoms are attained with the fullerene closest to the chloride anion of $Co(dppe)_2Cl$.

Fullerenes C_{70} form closely packed double chains arranged along the *a* axis in $\{Co(dppe)_2Cl\}(C_{70}) \cdot 0.5C_6H_4Cl_2$ (**2**). The

longer axis of C_{70} is directed along this axis, and the ctc interfullerene distance is 10.81 Å in this direction. The ctc interfullerene distance in the double chains along the *b* axis is 10.18 Å. As a result, multiple short vdW $C\cdots C$ contacts are formed between fullerenes (shown with green dashed lines in Fig. 4a). Double fullerene chains are completely isolated to give the ctc interfullerene distances among the neighboring double chains longer than 14 Å (Fig. 4b). Each $Co(dppe)_2Cl$ unit is surrounded by four C_{70} cages in **2** (Fig. 4c). In this case phenyl substituents cannot form a suitable cavity for a larger C_{70} ellipsoid, and it is positioned asymmetrically to $Co(dppe)_2Cl$ (Fig. 4c). There are no short $Cl(Co(dppe)_2Cl)\cdots C(C_{70})$ contacts in **2** unlike the crystal structure of **1**. The shortest $Co\cdots C(C_{70})$ distances are 5.94–6.70 Å.

The arrangement of ligands around cobalt atoms in the $Co(dppe)_2Cl$ units is similar in **1** and **2**. However, these units have different bond lengths at the cobalt atoms. The cobalt atoms are located in the pyramidal environment in both the units formed by four phosphorus atoms and one chloride anion. The Co atoms are not located strictly in the plane of four phosphorus atoms but move out of this plane by 0.110 and 0.124 Å towards chloride anion in **1** and **2**, respectively. The dimension of pyramidal coordination is informative to evaluate the charge on Co. As listed in Table 1, the average of Co–P length is increased according to the charge on Co (see, #0, 3–5).

The value of 2.2725(8) Å for **2** proves that Co is oxidized in this complex to almost +2, which corresponds well to a similar Co–Cl length to that of #3. On the contrary, the average Co–P length in **1** is shortened compared to those in Co^{II} materials.

Compared with that in #0, the Co in **1** is regarded not to be oxidized fully to +2. This evaluation corresponds well to the optical spectra and magnetic data for **1**.

Magnetic properties

Magnetic properties of **1** and **2** were studied by SQUID and EPR techniques. Effective magnetic moments of **1** and **2** are 1.98 and $2.27\mu_B$ at 300 K, respectively. These values are inter-

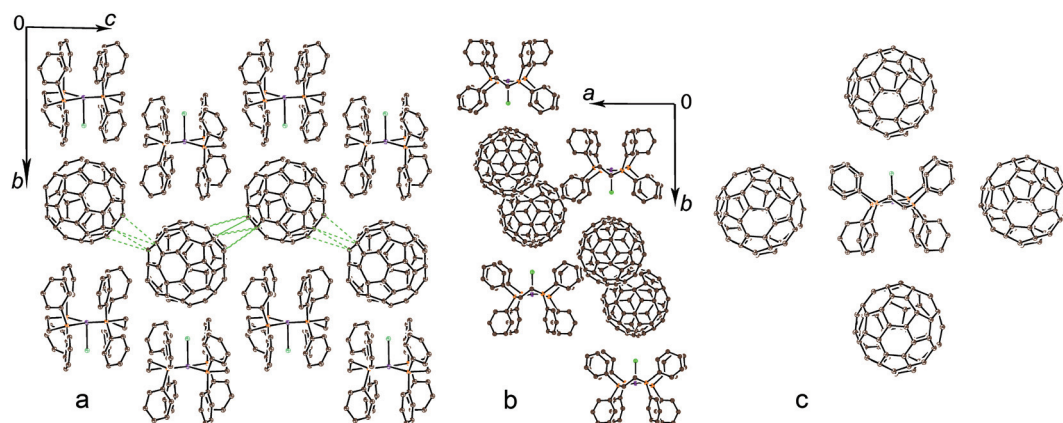


Fig. 3 (a) View of the crystal structure of **1** along the *a* axis and on zigzag C_{60} chains (shortened van der Waals $C\cdots C$ contacts between fullerenes are shown by green dashed lines) and (b) along the *c* axis and zigzag C_{60} chains; (c) $Co(dppe)_2Cl$ surrounded by four C_{60} cages. Only one of the two C_{60} orientations is shown.



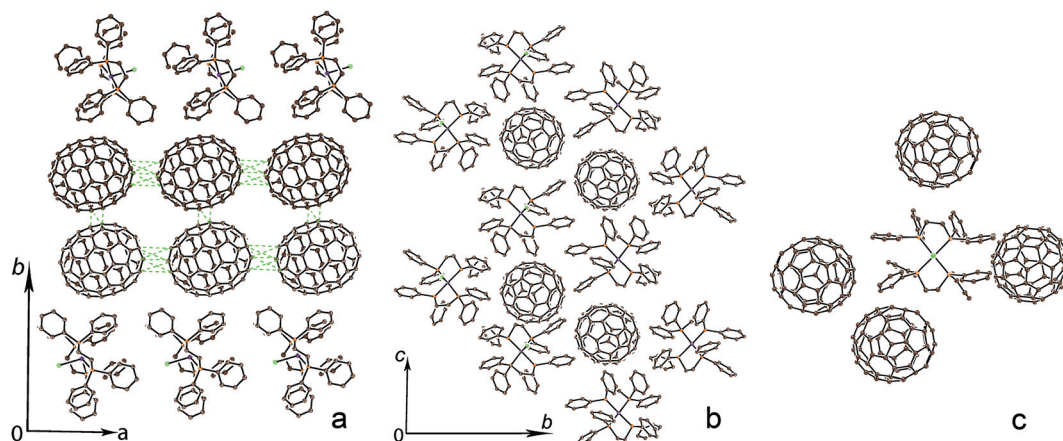


Fig. 4 (a) View of the crystal structure of **2** along the *c* axis and on double C_{70} chains (shortened van der Waals $C\cdots C$ contacts between fullerenes are shown by green dashed lines) and (b) along the *a* axis and double C_{70} chains; (c) surrounding of $Co(dppe)_2Cl$ by four C_{70} cages. Only major fullerene orientation is shown. Solvent molecules are not shown.

Table 1 Interatomic distances (Å) in $Co(dppe)_2L$ species

	Compound	Co–Cl	Co–P (average)	Ref.
#0	$\{Co^I(dppe)_2\}^+(C_{60}^{3-}) \cdot 2C_6H_4Cl_2$ (almost square planar)		2.193(2)	12
#1	$\{Co(dppe)_2Cl\}(C_{60})$ (1)	2.366(2)	2.2495(8)	This work
#2	$\{Co(dppe)_2Cl\}(C_{70}) \cdot 0.5C_6H_4Cl_2$ (2)	2.403(3)	2.2725(8)	This work
#3	$\{Co^{II}(dppe)_2Cl\}^+(SnCl_3^-) \cdot C_6H_5Cl$	2.398(2)	2.275(2)	28
#4	$\{Co^{II}(dppe)_2I\}^+(I^-) \cdot CHCl_3$		2.283(3)	29
#5	$\{Co^{II}(dppe)_2(CH_3CN)\}^{2+}(BF_4^-)_2 \cdot C_3H_6O$		2.306(3)	21

mediate between those characteristic of the systems of one and two non-interacting $S = 1/2$ spins per formula unit (1.73 and $2.45\mu_B$, respectively). In the case of **2**, the magnetic moment is closer to $2.45\mu_B$ than that of **1**. We suppose that paramagnetic $Co^{II}(dppe)_2Cl^+$ cations and C_{60}^{3-} or C_{70}^{3-} radical anions with the $S = 1/2$ spin state are formed in both complexes due to CT from $Co(dppe)_2Cl$ to fullerenes. Since the magnetic moment of $2.45\mu_B$ is expected in the fully charge-transferred $\{Co^{II}(dppe)_2Cl\}^+(fullerene)^{3-}$ state, the observed lower magnetic moments are most probably due to the coexistence of diamagnetic $\{Co^I(dppe)_2Cl\}^0(fullerene)^0$ with the total magnetic moments of $S = 0$. Moreover, magnetic moments are not constant at high temperature and increases above 220 K for **1** and 140 K for **2** (Fig. 5a and b). Such behavior can be explained by the increase of the degree of CT from $Co(dppe)_2Cl$ to fullerenes with temperature. The low-temperature part can be approximated well by the Curie–Weiss expression with Weiss temperatures of only -2 and -3.5 K for **1** and **2**, respectively (Fig. 5c and d). Thus, in spite of close packing of fullerenes in **1** and **2**, only weak antiferromagnetic coupling of spins and no long range ordering are observed in both complexes. The presence of neutral diamagnetic components and disordered fullerenes can interrupt the phase transition. Incomplete CT to fullerenes can also be the reason for the absence of fullerene dimerization in spite of their close packing in a crystal. Particularly, complex **2** should be noted

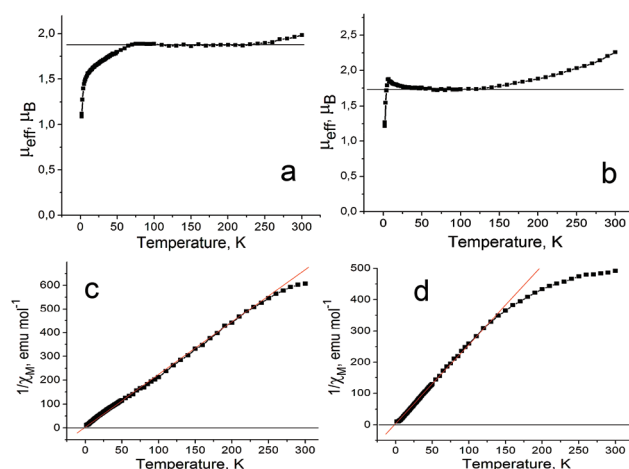


Fig. 5 Temperature dependencies for effective magnetic moments of **1** (a) and **2** (b), and reciprocal molar magnetic susceptibility of **1** (c) and **2** (d).

since the formation of stable singly bonded $(C_{70})_2$ dimers is observed in almost all the ionic compounds of C_{70} .^{17–19} The similar exceptional absence of dimerization was found for C_{60} complexes with partial CT states on average.³⁰

Complex **1** manifests an intense asymmetric EPR signal at room temperature which can be fitted well by three components with $g_1 = 2.0968$ (the linewidth (ΔH) of 15.51 mT),



$g_2 = 2.0488$ and $\Delta H = 11.06$ mT and $g_3 = 2.0085$ and $\Delta H = 8.16$ mT (Fig. 6a). The starting Co^{I} has $S = 1$ or most probably $S = 0$ spin state. Compounds of Co^{I} with the $S = 1$ spin state can manifest triplet EPR signals, for example, $\text{Co}^{\text{I}}(\text{Ph}_3\text{P})_3\text{X}$ ($\text{X} = \text{Cl}, \text{Br}$),³¹ but these signals cannot be observed by X-band EPR spectroscopy. Only high-frequency and -field EPR spectroscopy can be used for these purposes. Neutral fullerenes are EPR silent. Therefore, only the paramagnetic $\text{Co}^{\text{II}}(\text{dppe})_2\text{Cl}^+$ and the $\text{C}_{60}^{\cdot-}$ or $\text{C}_{70}^{\cdot-}$ radical anions can contribute to the EPR signals of **1** and **2**. Here, it is noted that the spin susceptibility estimated by the EPR signal intensity showed the same temperature dependency as that of magnetic susceptibility determined by the SQUID technique both for **1** and **2**. This means that there is no contribution of Co^{I} to the magnetism in these materials.

$\text{Co}^{\text{II}}(\text{dppe})\text{Br}_2$ shows the Lorentzian EPR signal with $g = 2.0357$ and $\Delta H = 15.5$ mT. However, $\text{Co}^{\text{II}}(\text{dppe})\text{Br}_2$ has tetrahedral geometry while the $\text{Co}^{\text{II}}(\text{dppe})_2\text{Cl}^+$ cations have the pyramidal environment for the cobalt atoms. Essential modification of the cobalt environment in the formation of $\text{Co}^{\text{II}}(\text{dppe})_2\text{Cl}^+$ can affect the EPR signal by shifting g -factors to higher values in comparison with that of $\text{Co}^{\text{II}}(\text{dppe})\text{Br}_2$. The signals with a g -factor closer to that of $\text{C}_{60}^{\cdot-}$ are also observed ($g_2 = 2.0488$ and $g_3 = 2.0085$) together with the signals characteristic of Co^{II} . These signals could be ascribed to both $\text{Co}^{\text{II}}(\text{dppe})_2\text{Cl}^+$ and $\text{C}_{60}^{\cdot-}$ species having exchange interaction. They are strongly narrowed with the temperature decrease (Fig. 6c) and grow in intensity with the temperature increase above 220 K. We attribute such behavior to the increase of the CT degree from $\text{Co}(\text{dppe})_2\text{Cl}$ to C_{60} . The component with $g_3 = 2.0980$ splits into two components below 40 K positioned at $g = 2.0979$ and 2.1501 . Both components shift to higher g -factors with the temperature decrease (Fig. 6b).

Complex **2** shows an intense EPR signal at room temperature which can be fitted by three Lorentzian lines with $g_1 =$

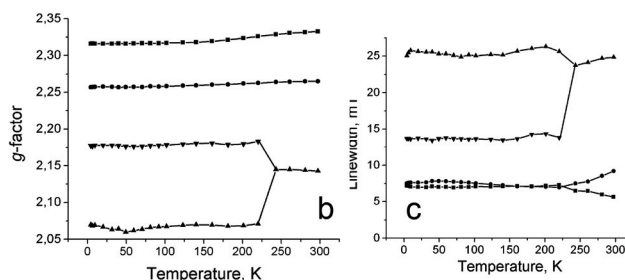
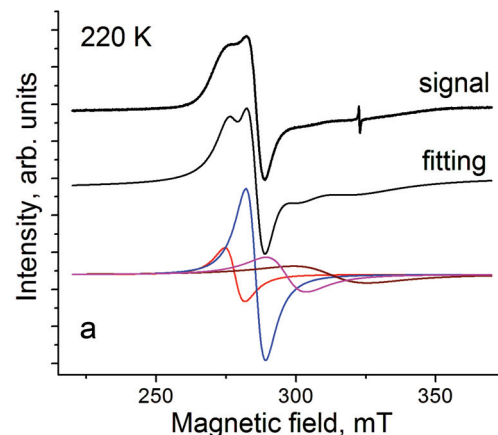


Fig. 7 EPR signal for polycrystalline **2** at 220 K (a); temperature dependence of the g -factor (b) and linewidth (c) of the components of the EPR signal of **2**.

2.3325 ($\Delta H = 5.62$ mT), $g_2 = 2.2649$ ($\Delta H = 9.20$ mT), and $g_3 = 2.1428$ ($\Delta H = 24.84$ mT) (Fig. 7). The broad g_3 -component splits into two lines below 220 K which are positioned at $g = 2.1829$ ($\Delta H = 13.86$ mT) and 2.0711 ($\Delta H = 25.64$ mT) at 220 K. Spectrum of **2** contains also weak narrow signal with $g = 2.0021$ ($\Delta H = 0.28$ mT) (Fig. 7a) which can appear due to air oxidation of fullerene anions. It is seen that the EPR signal in **2** is broader and has essentially higher g -factors of the lines in comparison with those of **1**. We can suppose that lines in the EPR spectrum of **2** with lower g -factors of 2.18 and 2.07 have essential contribution from $\text{C}_{70}^{\cdot-}$. It is known that the $\text{C}_{70}^{\cdot-}$ radical anions in $(\text{Ph}_4\text{P}^+)_2(\text{C}_{70}^{\cdot-})(\text{I}^-)$ show a broad EPR signal with a g -factor of 2.0047 ($\Delta H = 60$ mT) at 300 K.²⁷ Therefore, the lines in the spectrum of **2** originating from both $\text{Co}^{\text{II}}(\text{dppe})_2\text{Cl}^+$ and $\text{C}_{70}^{\cdot-}$ are essentially broader and shifted to higher g -factors in comparison with those of **1**. Lines with lower g -factors ($g = 2.18$ and 2.07) slightly grow in intensity with the temperature increase above 150 K and that can also be explained by the increase of the CT degree from $\text{Co}(\text{dppe})_2\text{Cl}$ to C_{70} .

Experimental

Materials

C_{60} of 99.9% purity and C_{70} of 99% purity were obtained from MTR Ltd and used without further purification. $\text{Co}^{\text{II}}(\text{dppe})\text{Cl}_2$ (98%) was purchased from Aldrich. Sodium fluorenone ketyl

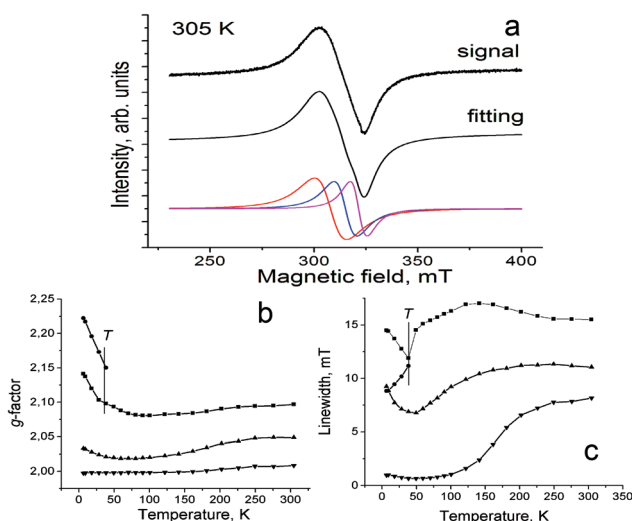


Fig. 6 (a) EPR signal for polycrystalline **1** at 305 K; temperature dependence of components of the EPR signal: (b) g -factor, (c) linewidth.



was obtained as described.³² Solvents were purified under an argon atmosphere and degassed. *o*-Dichlorobenzene (C₆H₄Cl₂) was distilled over CaH₂ under reduced pressure and hexane was distilled over Na/benzophenone. All manipulations for the syntheses of **1** and **2** were carried out in an MBraun 150B-G glove box with a controlled argon atmosphere and the content of H₂O and O₂ less than 1 ppm. The solvents and crystals were stored in the glove box. Polycrystalline samples of **1** and **2** were placed in 2 mm quartz tubes under anaerobic conditions for EPR and SQUID measurements and sealed under 10^{−5} torr pressure. KBr pellets for IR- and UV-visible-NIR measurements were prepared in the glove box.

Synthesis

Crystals of **1** and **2** were obtained by a diffusion technique. A reaction mixture was filtered into a 1.8-cm-diameter, 50 mL glass tube with a ground glass plug, and then 30 mL of hexane was layered over the solution. Slow mixing of the solutions resulted in precipitation of crystals over 1 month. The solvent was then decanted from the crystals, and they were washed with hexane. The compositions of the obtained salts were determined from X-ray diffraction analysis on a single crystal. Due to the high air sensitivity of **1** and **2**, elemental analysis could not be carried out to determine the composition because the salts reacted with oxygen in air before the quantitative oxidation procedure.

The crystals of {Co(dppe)₂Cl}(C₆₀) (**1**) and {Co(dppe)₂Cl}(C₇₀)-0.5C₆H₄Cl₂ (**2**) were obtained by the following procedure. The reduction of green Co^{II}(dppe)Cl₂ (22 mg, 0.042 mmol) in 16 ml of C₆H₄Cl₂ with sodium fluorenone ketyl (20 mg, 0.098 mmol) for 2 hours at 100 °C yielded a clear red solution. The solution was cooled down to room temperature and filtered into a flask containing fullerene C₆₀ (30 mg, 0.042 mmol) for preparation of **1** and fullerene C₇₀ (35 mg, 0.042 mmol) for preparation of **2**. Fullerenes were dissolved in the obtained solution over 4 hours at 80 °C to produce violet-red and red solutions, respectively. After cooling down to room temperature the solutions were filtered into the tube for diffusion. The crystals of {Co(dppe)₂Cl}(C₆₀) (**1**) were obtained as black plates in 26% yield together with black elongated parallelepipeds of the previously reported salt {Co^I(dppe)₂⁺}(C₆₀^{•−})-2C₆H₄Cl₂¹² (yield is 20%) which was identified by X-ray diffraction on several parallelepiped-shaped single crystals. The crystals of two phases have different shapes and were separated under a microscope in the glove box. The purity of **1** was supported by the absence of the line at *g* = 1.9986 (Δ*H* = 4.57 mT) characteristic of {Co^I(dppe)₂⁺}(C₆₀^{•−})-2C₆H₄Cl₂. The crystals of {Co(dppe)₂Cl}(C₇₀)-0.5C₆H₄Cl₂ (**2**) were obtained as black plates in 42% yield. Testing of several crystals from the synthesis shows the presence of only one phase in this synthesis.

General

UV-visible-NIR spectra were recorded using KBr pellets on a Perkin Elmer Lambda 1050 spectrometer in the 250–2500 nm range. FT-IR spectra were obtained using KBr pellets with a

Perkin-Elmer Spectrum 400 spectrometer (400–7800 cm^{−1}). EPR spectra were recorded for polycrystalline samples of **1** and **2** with a JEOL JES-TE 200 X-band ESR spectrometer equipped with a JEOL ES-CT470 cryostat working between room and liquid helium temperatures. A Quantum Design MPMS-XL SQUID magnetometer was used to measure the static magnetic susceptibility of **1** and **2** at 100 mT magnetic field under cooling and heating conditions in the 300–1.9 K range. The sample holder contribution and core temperature independent diamagnetic susceptibility (χ_d) were subtracted from the experimental values. The χ_d values were estimated by the extrapolation of the data in the high-temperature range by fitting the data with the following expression: χ_M = *C*/(*T* − Θ) + χ_d, where *C* is the Curie constant and Θ is the Weiss temperature. The effective magnetic moment (μ_{eff}) was calculated with the formula μ_{eff} = (8χ_M*T*)^{1/2}.

Crystal structure determination

The intensity data for **1** and **2** were collected on an IPDS (Stoe) diffractometer with graphite monochromated Mo-Kα radiation (λ = 0.71073 Å). The structures were solved by a direct method and refined by a full-matrix least-squares method against *F*² using SHELXL 2014/7.³³ All non-hydrogen atoms were refined anisotropically. Positions of hydrogen atoms were included into refinement in a riding model. See the ESI† for crystallographic data in CIF format.

Crystal data of **1** at 100(2) K: C₁₁₂H₄₈ClCoP₄, *M*_r = 1611.76 g mol^{−1}, black plate, monoclinic, *C*2/*c*, *a* = 22.1120(6), *b* = 19.1090(6), *c* = 17.0090(4) Å, β = 107.480(2)°, *V* = 6855.1(3) Å³, *Z* = 4, *d*_{calc} = 1.562 g cm^{−3}, μ = 0.446 mm^{−1}, *F*(000) = 3296, 2θ_{max} = 58.4°, reflections measured 36 820, unique reflections 9002, reflections with *I* > 2σ(*I*) = 6591, parameters refined 630, restraints 180, *R*₁ = 0.0735, *wR*₂ = 0.1851, G.O.F. = 1.083. The C₆₀ cage is disordered over two orientations linked by a two-fold axis. CCDC 1437134.

Crystal data of **2** at 100(2) K: C₁₂₅H₅₀Cl₂CoP₄, *M*_r = 1805.36 g mol^{−1}, black plate, monoclinic, *P*2₁/*n*, *a* = 10.8104(3), *b* = 39.8917(10), *c* = 18.2142(5) Å, β = 100.133(2)°, *V* = 7732.3(4) Å³, *Z* = 4, *d*_{calc} = 1.551 g cm^{−3}, μ = 0.438 mm^{−1}, *F*(000) = 3684, max. 2θ_{max} = 53.5°, reflections measured 47 143, unique reflections 15 869, reflections with *I* > 2σ(*I*) = 10 991, parameters refined 821, restraints 24, *R*₁ = 0.0814, *wR*₂ = 0.2035, G.O.F. = 1.000. The C₇₀ cage is disordered between three orientations with the 0.45/0.30/0.25 occupancies. The solvent C₆H₄Cl₂ molecule is statistically disordered between two orientations. CCDC 1437135.

Conclusions

The interaction of the Co^I species generated by the reduction of Co^{II}dppeCl₂ allows the preparation of CT complexes {Co(dppe)₂Cl}(C₆₀) (**1**) and {Co(dppe)₂Cl}(C₇₀)-0.5C₆H₄Cl₂ (**2**). Both complexes contain the C₆₀^{•−} or C₇₀^{•−} radical anions and the Co^{II}(dppe)₂Cl⁺ cations formed as a result of CT from Co^I(dppe)₂Cl to fullerenes. CT becomes possible due to the



strong donor properties of $\text{Co}^{\text{I}}(\text{dppe})_2\text{Cl}$ which are enough to produce fullerene $^{\cdot-}$ radical anions. However, most probably CT is not complete and diamagnetic $\{\text{Co}^{\text{I}}(\text{dppe})_2\text{Cl}\}^0$ and neutral fullerenes are also preserved in the samples. As a result, in spite of the close packing of fullerenes in the chains only weak magnetic coupling of spins is observed and fullerenes are not dimerized in both complexes. The absence of dimerization allows for the first time to observe the solid state optical spectrum of monomeric $\text{C}_{70}^{\cdot-}$ radical anions and to determine their molecular structure. It is also seen that organometallic compounds with strong donor properties can be promising components to design fullerene complexes with partial CT.

Acknowledgements

The work was supported by the Russian Science Foundation (project no. 14-13-00028) and by JSPS KAKENHI Grant Numbers 23225005 and 26288035.

Notes and references

- 1 K. Tanigaki and K. Prassides, *J. Mater. Chem.*, 1995, **5**, 1515.
- 2 P. W. Stephens, G. Bortel, G. Faigel, M. Tegze, A. Jánossy, S. Pekker, G. Oszlanyi and L. Forró, *Nature*, 1994, **370**, 636.
- 3 D. V. Konarev, S. S. Khasanov, A. Otsuka, M. Maesato, G. Saito and R. N. Lyubovskaya, *Angew. Chem., Int. Ed.*, 2010, **49**, 4829.
- 4 P. W. Stephens, D. Cox, J. W. Lauher, L. Mihaly, J. B. Wiley, P.-M. Allemand, A. Hirsch, K. Holczer, Q. Li, J. D. Thompson and F. Wudl, *Nature*, 1992, **355**, 331.
- 5 D. V. Konarev and R. N. Lyubovskaya, *Russ. Chem. Rev.*, 2012, **81**, 336.
- 6 C. A. Reed and R. D. Bolskar, *Chem. Rev.*, 2000, **100**, 1075.
- 7 W. C. Wan, X. Liu, G. M. Sweeney and W. E. Broderick, *J. Am. Chem. Soc.*, 1995, **117**, 9580.
- 8 D. V. Konarev, S. S. Khasanov, G. Saito, A. Otsuka, Y. Yoshida and R. N. Lyubovskaya, *J. Am. Chem. Soc.*, 2003, **125**, 10074.
- 9 D. V. Konarev, S. S. Khasanov, I. I. Vorontsov, G. Saito, Yu. M. Antipin and R. N. Lyubovskaya, *Inorg. Chem.*, 2003, **42**, 3706.
- 10 C. Bossard, S. Rigaut, D. Astruc, M.-H. Delville, G. Félix, A. Février-Bouvier, J. Amiell, S. Flandrois and P. Delhaès, *J. Chem. Soc., Chem. Commun.*, 1993, 333.
- 11 D. V. Konarev, S. S. Khasanov, A. Otsuka, H. Yamochi, G. Saito and R. N. Lyubovskaya, *Inorg. Chem.*, 2014, **53**, 6850.
- 12 D. V. Konarev, A. V. Kuzmin, S. V. Simonov, S. S. Khasanov, E. I. Yudanov and R. N. Lyubovskaya, *Dalton Trans.*, 2011, **40**, 4453.
- 13 M. Schulz-Dobrick and M. Jansen, *Angew. Chem., Int. Ed.*, 2008, **47**, 2256.
- 14 D. V. Konarev, S. S. Khasanov, S. I. Troyanov, Y. Nakano, K. A. Ustimenko, A. Otsuka, H. Yamochi, G. Saito and R. N. Lyubovskaya, *Inorg. Chem.*, 2013, **52**, 13934.
- 15 D. V. Konarev, S. I. Troyanov, Y. Nakano, K. A. Ustimenko, A. Otsuka, H. Yamochi, G. Saito and R. N. Lyubovskaya, *Organomet.*, 2013, **32**, 4038.
- 16 D. V. Konarev, S. I. Troyanov, K. A. Ustimenko, Y. Nakano, A. F. Shestakov, A. Otsuka, H. Yamochi, G. Saito and R. N. Lyubovskaya, *Inorg. Chem.*, 2015, **54**, 4597.
- 17 D. V. Konarev, S. S. Khasanov, I. I. Vorontsov, G. Saito, Yu. A. Antipin, A. Otsuka and R. N. Lyubovskaya, *Chem. Commun.*, 2002, 2548.
- 18 D. V. Konarev, S. S. Khasanov, S. V. Simonov, E. I. Yudanov and R. N. Lyubovskaya, *CrystEngComm*, 2010, **12**, 3542.
- 19 D. V. Konarev, A. V. Kuzmin, S. V. Simonov, S. S. Khasanov, A. Otsuka, H. Yamochi, G. Saito and R. N. Lyubovskaya, *Dalton Trans.*, 2012, **41**, 13841.
- 20 D. Dubois, K. M. Kadish, S. Flanagan, R. F. Haufler, L. P. F. Chibante and L. J. Wilson, *J. Am. Chem. Soc.*, 1991, **113**, 4364.
- 21 R. Ciancanelli, B. C. Noll, D. L. DuBois and M. R. DuBios, *J. Am. Chem. Soc.*, 2002, **124**, 2984.
- 22 K. Kuwata and D. H. Geske, *J. Am. Chem. Soc.*, 1964, **86**, 2101.
- 23 R. O. Loutfy, K. Hsiaob, S. Ong and B. Keoshkeria, *Can. J. Chem.*, 1984, **62**, 1877.
- 24 T. Picher, R. Winkler and H. Kuzmany, *Phys. Rev. B: Condens. Matter*, 1994, **49**, 15879.
- 25 V. N. Semkin, N. G. Spitsina, S. Krol and A. Graja, *Chem. Phys. Lett.*, 1996, **256**, 616.
- 26 D. V. Konarev, N. V. Drichko and A. Graja, *J. Chim. Phys.*, 1998, **95**, 2143.
- 27 A. Penicaud, A. P. Perez-Benitez, R. Escudero and C. Coulon, *Solid State Commun.*, 1995, **96**, 147.
- 28 J. K. Stalick, P. W. R. Corfield and D. W. Meek, *Inorg. Chem.*, 1973, **12**, 1668.
- 29 S. Aizawa, K. Fukumoto and T. Kawamoto, *Polyhedron*, 2013, **62**, 37.
- 30 D. V. Konarev, S. S. Khasanov, M. Ishikawa, E. I. Yudanov, A. F. Shevchun, M. S. Mikhailov, P. A. Stuzhin, A. Otsuka, H. Yamochi, G. Saito and R. N. Lyubovskaya, *Chem. Select*, 2016, **1**, 323.
- 31 J. Krzystek, A. Ozarowski, S. A. Zvyagin and J. Telser, *Inorg. Chem.*, 2012, **51**, 4954.
- 32 D. V. Konarev, S. S. Khasanov, E. I. Yudanov and R. N. Lyubovskaya, *Eur. J. Inorg. Chem.*, 2011, 816.
- 33 G. M. Sheldrick, *Acta Crystallogr., Sect. A: Fundam. Crystallogr.*, 2008, **64**, 112.

